

Article

Spatio-Temporal Dynamic of the Land Use/Cover Change and Scenario Simulation in the Southeast Coastal Shelterbelt System Construction Project Region of China

Shengwang Bao and Fan Yang *

School of Economics and Management, Zhejiang Ocean University, Zhoushan 316022, China;
bao_shengwang@163.com

* Correspondence: yang-fan@zjou.edu.cn

Abstract: The National Coastal Shelterbelt System Construction Project (NCSSCP) was proposed to increase the afforestation area and neutralize the impact of urbanization, especially in the southeast coastal sub-region of China. In this study, we identified the spatio-temporal evolution characteristics and predicted the land use and land cover changes (LUCC) associated with this project by modeling scenarios, seeking to explore the path of sustainable development. The spatial structure was analyzed using the landscape pattern index approach and the land use transfer matrix. By coupling the Markov model and patch-generating a land-use simulation model (PLUS), different scenarios were analyzed to predict the quantity and spatial changes. According to the results, based on the current trends and due to the impact of urbanization, the forest area was predicted to decrease by 633.19 km², whilst appearing more spatially fragmented and separated. However, with the completion of the NCSSCP target, the forest area was predicted to increase by 1666.12 km², and the spatial structure would appear more cohesive and concentrated. From an overall perspective, the afforestation target of NCSSCP will not be completed under the present trend. It is difficult for the afforestation speed of the NCSSCP to keep up with the speed of urbanization. Therefore, giving consideration to both the afforestation speed and quality and reducing the speed of urbanization to balance the economy and ecology would be beneficial in terms of the realization of the aims of sustainable development.

Keywords: LUCC; spatio-temporal analysis; NCSSCP; PLUS; scenario prediction



Citation: Bao, S.; Yang, F. Spatio-Temporal Dynamic of the Land Use/Cover Change and Scenario Simulation in the Southeast Coastal Shelterbelt System Construction Project Region of China. *Sustainability* **2022**, *14*, 8952. <https://doi.org/10.3390/su14148952>

Academic Editor: Irene Petrosillo

Received: 14 June 2022

Accepted: 11 July 2022

Published: 21 July 2022

Publisher's Note: MDPI stays neutral with regard to jurisdictional claims in published maps and institutional affiliations.



Copyright: © 2022 by the authors. Licensee MDPI, Basel, Switzerland. This article is an open access article distributed under the terms and conditions of the Creative Commons Attribution (CC BY) license (<https://creativecommons.org/licenses/by/4.0/>).

1. Introduction

With rapid economic development, the rapid urbanization process in coastal areas has led to a series of land use issues such as soil erosion [1], forest reduction [2] and other environmental problems which severely threaten the economic development of coastal areas. In 1988, the National Coastal Shelterbelt System Construction Project (NCSSCP) was first proposed. From 1991 to 2000, the construction of the coastal shelter forest system was fully implemented in 11 coastal provinces across China. In 2001, the State Forestry Administration organized the NCSSCP Phase II Plan (2001–2010). The second period was extended to 2015, further expanding the scope of the project's construction. In 2015, the implementation of the previous phase of the plan came to an end. The third phase of the NCSSCP (2016–2025) [3] was then launched. The goals of NCSSCP phase III can be divided according to their function into basal forest belt construction and deep forest belt construction, and can be divided into 11 coastal provinces according to their region. The southeast coastal area mainly includes the southeastern sections of Zhejiang Province, some districts and counties of Ningbo City, and Fujian Province. Unclear zoning areas were distributed according to the proportion of forest area, and the target afforestation area of the NCSSCP was 1698.42 km².

The southeastern coastal area has a subtropical monsoon climate, with abundant precipitation, sufficient sunlight, diverse terrain, rich resources, and dense woodland;

enormous achievements have been obtained in this area under the influence of the NCSSCP. However, there are still problems to be solved urgently, such as the low positioning, deficiency in the total amount, and insufficient width of forest belts, as well as their unreasonable structure [4]. Moreover, the level of NCSSCP forest construction still lags behind the levels of economic and social construction, and relevant research is urgently required.

Many ecosystem and environmental degradation issues have induced fluctuations in urban temperatures [5] and the eutrophication of the sea with the acceleration of urbanization [6]. The expansion of construction land occupies the area of agricultural land. Therefore, it is difficult to ensure economic growth and living necessities due to more severe land-use conflicts. The use of empirical models [7], the analysis of conflict zones [8], and spatial identification and intensity diagnosis models for potential land use functions [4] can reflect the real situation of land use and land cover changes (LUCC). Hence, the regression method [9] and the decision tree model [10] of the random forest algorithm were employed here to boost the accuracy of the LUCC, so as to improve the spatial resolution of the southeastern coastal area for the following in-depth research. Because the expansion of urban areas has resulted in unbalanced forest displacement [11] and tremendous pressure on forest land, the Chinese government developed the NCSSCP [12]. The effects of the NCSSCP have been analyzed in many studies from different perspectives. Researchers have analyzed soil microbial and enzyme activities in order to breed tree species which are suitable for shelterbelts [13], and have adopted spatial domain effect models to assess the spatio-temporal patterns of shelterbelts [14]. The effects of the NCSSCP were demonstrated by calculating the total primary productivity of forest vegetation [15], and by quantifying the structure and plant diversity of shelterbelts [12]. Moreover, the ecological and environmental impacts of the NCSSCP were explored from the perspective of ecosystem protection and function [16,17]. Under the influence of the NCSSCP in the southeastern coastal area, modeling scenarios and the simulation of the spatio-temporal evolution of LUCC can reveal changes in spatial patterns and assist decision-makers in formulating sustainable development strategies. Thus, two questions were proposed in this study:

1. Can the shelterbelt construction project successfully complete its goals according to the development trends of the third phase of the NCSSCP?
2. What is the most suitable land resource management and planning strategy for the southeastern coastal area?

LUCCs affect the landscape pattern and spatial structure [18]. The distribution characteristics of LUCCs can be recognized by selecting appropriate landscape pattern indexes, and by quantitatively analyzing the spatial structure [19]. Therefore, the high-quality development of coastal cities and the management of land resources should be strengthened by analyzing the characteristics of LUCCs and predicting the spatio-temporal evolution trends of LUCCs under different scenarios [20]. Regional LUCCs consist of both quantitative changes and evolutions in the spatial structure, and the chosen model must have both quantitative prediction and spatial simulation capabilities [21]. Existing quantitative prediction models consist of univariate gray models [22], system dynamics models [23], logistic regression models [24], Markov models [25], and artificial neural network models [26]. The Markov model describes stochastic processes based on Markov chain theory [27], and is widely used in land use simulation prediction due to its lack of after-effects. The cellular automaton model can simulate LUCC according to certain conversion rules [28], based on the CA-Markov model [29], the CLUE-S model [30], the FLUS model [31], and the ST-CA model [32], which are broadly applied to LUCC spatio-temporal evolution simulations. However, they possess a weak ability to mine the potential drivers of LUCC and the use of multiple patch types. Through the land expansion analysis strategy, the patch-generating land use simulation (PLUS) model can be used to find the intrinsic driving force of the spatio-temporal evolution of LUCC [33]. Combined with multi-objective optimization algorithms, the PLUS model simulates the spatio-temporal evolution of LUCC at a higher accuracy with new multiple random seed generation mechanisms.

Therefore, the spatio-temporal evolution trend of the LUCC and the spatial pattern in the southeastern coastal area from 1990 to 2020 are analyzed in this paper. Besides this, the LUCC in 2020 is simulated by coupling the Markov quantity prediction model and the PLUS model based on the remote sensing images of the LUCC in 2010 and 2015, and the appropriate drivers. The Kappa coefficient is an indicator used for consistency testing, and can also be used to measure the effect of classification. Therefore, the kappa coefficient indicator is employed to verify the accuracy of the Markov-PLUS model. According to the NCSSCP, the inertial development scenario and the goal-oriented scenario are set to predict the evolution trend of the LUCC. Additionally, a suitable landscape pattern index system is established to analyze the spatial structure and provide a scientific basis for the subsequent sustainable development in the southeastern coastal area. The inspection of the NCSSCP results can provide a reference for the completion of the project's objectives, land resource planning management, and sustainable development in the southeastern coastal area.

2. Study and Data Sources

2.1. Study Area

Located at $24^{\circ}52' \sim 31^{\circ}04' \text{ N}$, $117^{\circ}35' \sim 123^{\circ}25' \text{ E}$ (Figure 1), the southeastern coastal area spans the Zhejiang and Fujian provinces, including 79 coastal cities and a total area of 83,600 km^2 . The southeastern coastal area is one of the ten major ecological barriers and major ecological restoration projects. The terrain of the southeastern coastal area is dominated by medium and low mountains and hills. Bounded by provincial administrative divisions, the terrain of Zhejiang slopes from the southwest to the northeast, while the terrain of Fujian slopes from the northwest to the southeast. The southeastern coastal area belongs to the subtropical monsoon climate, presenting sufficient sunshine and abundant rainfall, with an average annual temperature of about 17°C and an average annual precipitation of 1200–2000 mm. The type of soil is generally laterite and yellow soil, and the vegetation type is dominated by subtropical evergreen broad-leaved forest in the central and western regions, and subtropical monsoon forest in the east. The construction of shelterbelts along the southeastern coastal area takes place in three areas: the Zhoushan bedrock coastal island area, the southeast Zhejiang and eastern Fujian bedrock coastal mountainous and hilly area, and the southern Fujian sandy silt coastal and hilly area. With a total population of 48.455 million people and a rapid rate of urbanization, the southeastern coastal shelterbelt construction area is one of the most economically developed areas in China. It is also the 'locomotive' driving China's economic and social development, and plays a pivotal role in the overall situation of national economic and social development.

2.2. Data Resources

The research data selected in this paper can be classified into natural environmental data, socioeconomic data, LUCC data, and planning documents according to their attributes (Table 1). Among these, the slope and aspect data of the natural environment data were mainly produced using ArcMap 10.8, which is based on DEM data; the restricted data were extracted from the water area data of the LUCC in 2020. In 2015, the State Forestry Administration and the National Development and Reform Commission issued the "National Coastal Shelter Forest System Construction Project Planning (2016–2025)", which has guiding significance for the construction of the southeastern coastal shelter forest system.

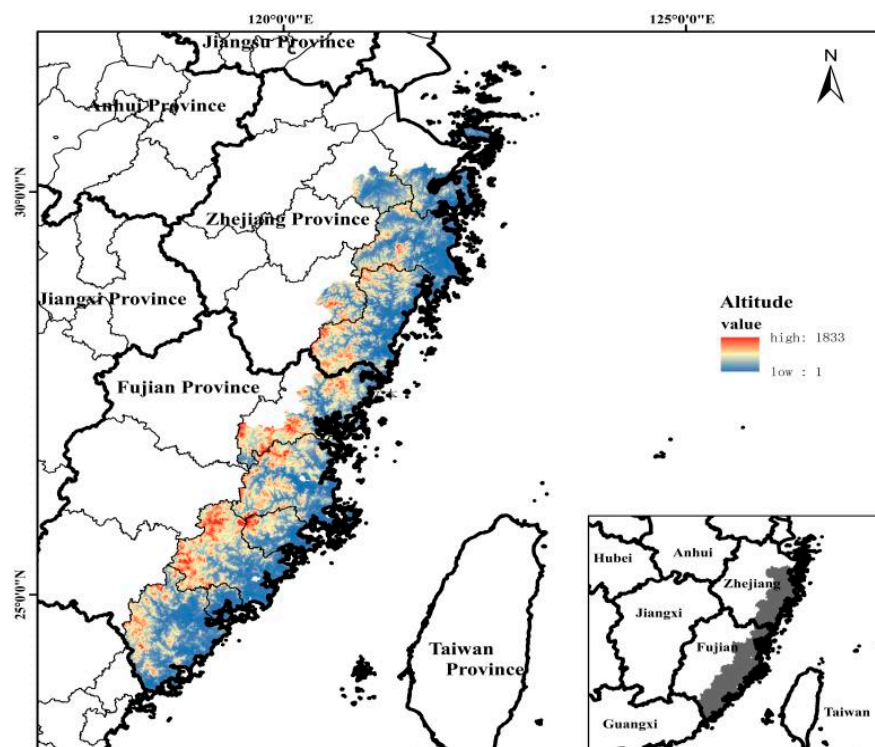


Figure 1. Study area.

Table 1. A list of the data used in the study.

Category	Data	Sources	Spatial Resolution
Natural environment data	DEM, slope, aspect	Geospatial data cloud (http://www.gscloud.cn/) (accessed on 16 March 2022)	30 m
	Precipitation	National Earth Systems Science Data Center (http://loess.geodata.cn) (accessed on 16 March 2022)	30 m
Socioeconomic data	GDP	Resource and Environmental Science Data Center (http://www.resdc.cn) (accessed on 17 March 2022)	30 m
	Distance to Build-up Area	Scientific data bank (https://www.scidb.cn) (accessed on 20 March 2022)	1000 m
	Distance to Residential Sites	National Geographic Information Resources Directory Service System (https://www.webmap.cn/) (accessed on 20 March 2022)	30 m
	Distance to Coastline	National Geographic Information Resources Directory Service System (https://www.webmap.cn/) (accessed on 21 March 2022)	30 m

Table 1. Cont.

Category	Data	Sources	Spatial Resolution
LUCC	LUCC data in 1990, 1995, 2000, 2005, 2010, 2015, 2020	CLCD from Wuhan University [34]	30 m
Limit development data	Water area	-	-
Plan file	National Coastal Shelterbelt System Construction Project Planning	The Central People's Government of the People's Republic of China (http://www.gov.cn/) (accessed on 1 March 2022)	-

3. Methodology

3.1. Landscape Pattern Index

The landscape pattern index is a crucial research tool for the analysis of the spatial characteristics [35] and the spatial distribution of its landscape structure [36]. The landscape index in this study is derived from two dimensions of landscape fragmentation and landscape diversity, in accordance with the actual situations of the study area. The landscape fragmentation indicators primarily consist of the landscape shape index (LSI), contagion (CONTAG), and land division index (DIVISION). The landscape diversity indicators comprise the agglomeration index (AI), Shannon's diversity index (SHDI), and Shannon's mean index (SHEI). The selected landscape pattern index and its formula are listed in Table 2.

Table 2. The landscape pattern index chosen in this study.

Landscape Pattern Index	Relation	Formulation
Landscape fragmentation indicators	LSI	The larger the value, the more complex the shape of landscape patch and the higher the degree of landscape fragmentation. $LSI = \frac{0.25 \sum_{ij}^n e_{ij}^*}{\sqrt{TA}}$
	CONTAG	The larger the value, the higher the agglomeration degree between landscape patches, and the lower the landscape fragmentation degree. $CONTAG = \left[1 + \left(\sum_{i=1}^n \sum_{j=1}^n (p_i) \left(\frac{f_{ij}}{\sum_{i=1}^n f_{ij}} \right) \right) \left[\ln(p_i) \frac{f_{ij}}{\sum_{i=1}^n f_{ij}} \right] \right] \div 2 \ln(n) \times 100$
	DIVISION	The higher the degree of separation, the higher the degree of dispersion and fragmentation of the landscape system. $p_i = \frac{D_{ij}}{M_{ij}}$
Landscape diversity indicators	AI	The larger the value, the more the same landscape patches gather, and the lower the landscape fragmentation degree. $AI = \left[\frac{g_{ij}}{\max \rightarrow g_{ij}} \right]$
	SHDI	The larger the value, the more heterogeneous the patches in the landscape pattern, and the more fragmented the landscape. $SHDI = - \sum_{i=1}^n (p_i \ln p_i)$
	SHEI	The closer the value is to 1, the more evenly distributed the patchwork types are in landscape pattern. $SHEI = \frac{- \sum_{i=1}^n (p_i \ln p_i)}{\ln(n)}$

The LSI indicates the shape of the landscape patches, and its value is positive for landscape fragmentation. CONTAG describes the degree of agglomeration or the extension trend of patch types in the landscape, and is inversely proportional to the landscape fragmentation. The value of DIVISION is positive for fragmented landscapes. The AI shows the agglomeration degree of a certain type of landscape element type patch. SHDI suggests that the landscape elements are dominated by a few dominant patch types. In particular, the larger values represent more heterogeneous patches. SHEI reveals that the landscape elements are dominated by a few dominant patchwork types, and its value is inversely positive to the diversity.

3.2. Markov Model

The Markov model has high simulation accuracy in the process of simulating land use and land cover, and presents a lack of after-effects, in that LUCC is only related to

the previous moment and is not related to the later moment [37]. Therefore, this paper selects the Markov model to simulate the LUCC of 2020 in the southeastern coastal area on the basis of the remote sensing images of 2010 and 2015. The results were compared with the real images of 2020 in order to check the accuracy of the model. Besides this, the quantity of the LUCC in the southeastern coastal area in 2020 was predicted by using the Markov model based on the remote sensing images of 2010 and 2015. The results were compared with the real images of 2020 in order to check the accuracy of the model. The inertial development scenario and the goal-oriented are utilized in this study. In the inertial development scenario, the LUCC images from 2015 to 2020 were utilized to create the Markov model to predict the LUCC in 2025. In the goal-oriented scenario, the land-use evolution and distribution characteristics in 2025 were simulated under the forest land construction target of the NCSSCP.

3.3. PLUS Model

The patch-generating land-use simulation model (PLUS) is a land-use simulation model developed by the HPSCIL@CUG laboratory of the China University of Geosciences [38]. With raster data, the PLUS model can flexibly handle multiple types of land use patch changes, and can be used for patch-scale land-use change simulations [39]. The PLUS model combines the advantages of the transformation analysis strategy and the pattern analysis strategy to form the Land Use Expansion Analysis Strategy (LEAS) [40]. By extracting part of the land use expansion with two phases of the LUCC images, LEAS digs deep into the land-use conversion rules and obtains the conversion inertia probability of each category [41]. A CA model based on multi-type random patch seeds (CARS) [42] is proposed to automatically simulate and generate land use patches under the spatiotemporal state with the constraints of development land. The PLUS model couples the Land Use Expansion Analysis Strategy (LEAS) and the CA Model (CARS) based on multi-type random patch seeds, and combines the random seed generation and threshold decreasing mechanism to accurately simulate the LUCC [43]. Compared with the current land use simulation models, such as CA-Markov and logistics-CA, which use transformation analysis strategies, as well as CLUE-S and FLUS, which use pattern analysis strategies [44], the PLUS model has the following advantages: (1) PLUS can better explore the incentives of various types of land-use changes; (2) CARS can better simulate the patch-level changes of multiple types of land use; (3) the simulation results can better support planning policy in combination with multi-objective optimization algorithms.

The land-use expansion data from 2015 to 2020 are extracted when the PLUS model is used for simulation. Among them, 20% of the data are extracted by a random sampling strategy as the training set with the random forest algorithm. The contribution value of each driving factor is calculated in order to obtain the development probability atlas of various types of land use by LEAS. In this way, the probability of random seeds is determined to be 0.01 in order to simulate future types of land use patches (CARS). The land use transfer matrix refers to the land transfer from 2015 to 2020, and the construction land will not be transferred out due to its particularity. The neighbourhood weight is confirmed by referring to the ratio of the transfer area to the total transfer area of each category of land use in the past land transfer changes (see Table 3).

Table 3. The transition matrix and neighborhood weights.

The Type of Land Use	Cropland	Forest	Grassland	Water Area	Bare Land	Construction Land	Wetland
cropland	1	1	1	1	0	1	0
forest	1	1	0	0	0	1	0
grassland	1	0	1	1	0	1	0
water area	1	0	0	1	0	1	0
bare land	1	0	1	0	1	1	0
construction land	0	0	0	0	0	1	0
wetland	0	0	0	1	0	1	1
Neighborhood Weights	0.2	0.395	0.05	0.15	0.025	0.155	0.025

This section is divided into subheadings, providing a concise and precise description of the experimental results, their interpretation, and the experimental conclusions that can be drawn. The workflow chart is shown in Figure 2.

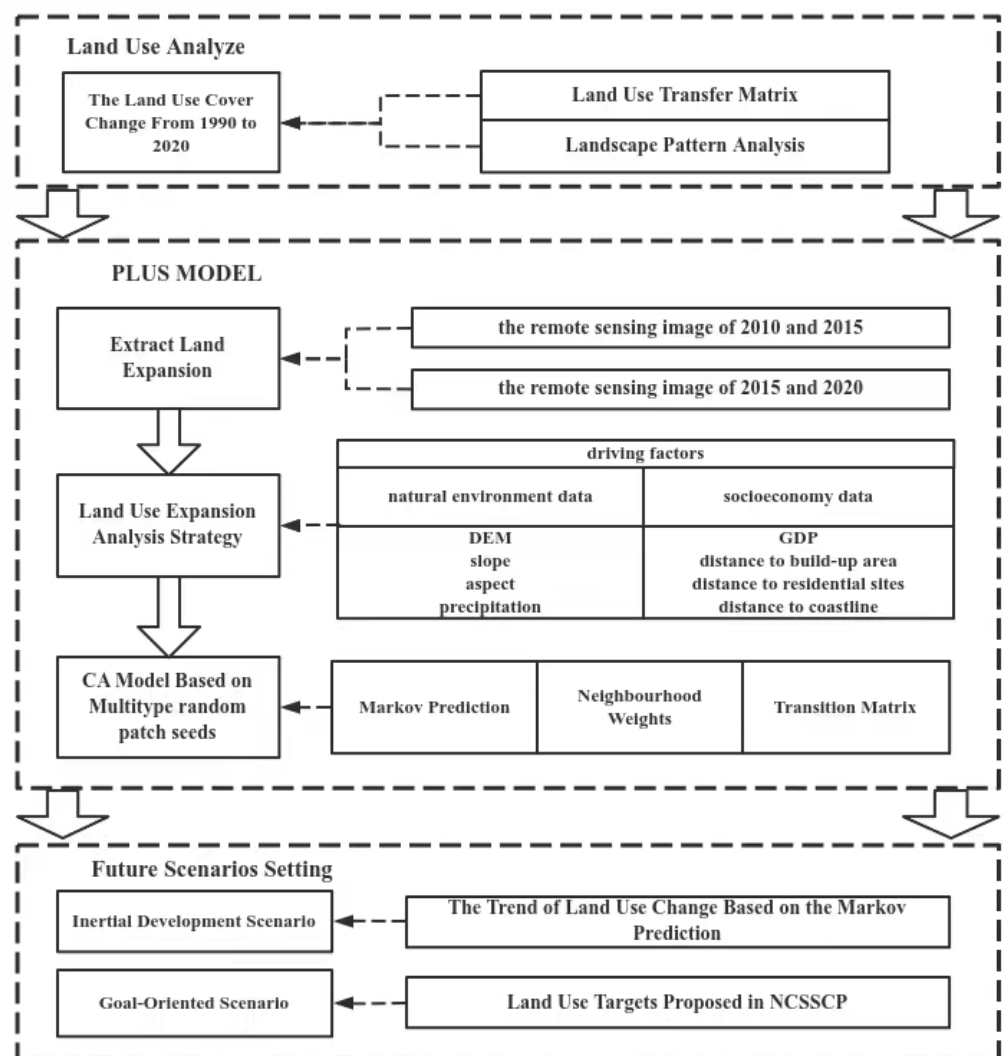


Figure 2. The workflow chart of this study.

3.4. Verification of the Kappa Index

The confusion matrix was employed to verify the simulation result image and compare its accuracy. The confusion matrix classifies the simulated remote sensing images and calculates the error matrix by comparing them with the real remote sensing images.

Concurrently, the confusion matrix was composed of three accuracy indicators: overall accuracy, producer accuracy, and user accuracy [45]. The Kappa coefficient comprehensively considers all factors and reflects the accuracy of the simulation. The Kappa coefficient was positively correlated with the simulation accuracy. Generally, the simulation effect and the performance were preferable when the Kappa coefficient belonged to (0.8, 1) [46].

In this paper, the remote sensing images of the LUCC in 2010 and 2015 were adopted. The remote sensing images of the LUCC in 2020 were simulated using PLUS by extracting land-use expansion and making various types of land use development possibility images according to LEAS. The quantity of the LUCC was predicted by using the CARS module. Compared with the real LUCC remote sensing images in 2020, the Kappa coefficient accuracy was 0.891 and the overall accuracy was 0.951. The fitting results of the model met the simulation requirements.

3.5. Selection of the Driving Factors

Socioeconomic data and natural environmental data were selected as driving factors, including the DEM, slope, aspect, GDP, precipitation, distance to the coastline, distance to a built-up area, and distance to residential sites (Figure 3). The missing part of the data was supplemented by interpolation, and the resampling was unified to a 30-m resolution. The driving factors were put into the LEAS in order to extract the development probability of each type of land use.

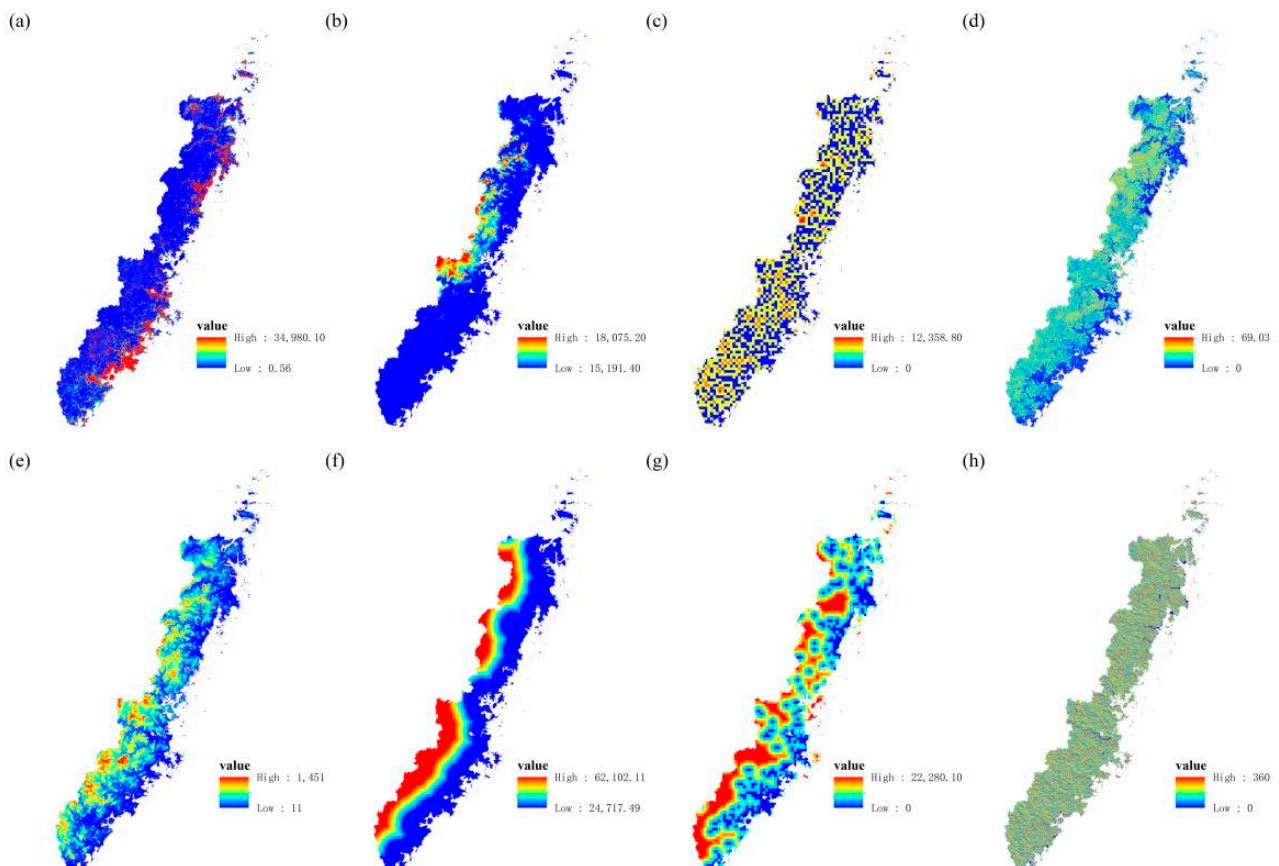


Figure 3. The driving factor chosen in this study. (a) the driving factor of GDP; (b) the driving factor of precipitation; (c) the driving factor of distance to residential sites; (d) the driving factor of slope; (e) the driving factor of Dem; (f) the driving factor of distance to coastline; (g) the driving factor of distance to build-up area; (h) the driving factor of aspect.

The random forest algorithm was utilized to mine the contribution value of each driving factor to the expansion of each type of land use. A total of two simulation plans were carried out in this paper.

1. LUCC remote sensing images from 2010 to 2015 were used to simulate the LUCC in 2020 for the Kappa coefficient verification.
2. LUCC remote sensing images from 2015 to 2020 were employed to simulate the LUCC under the effect of the NCSSCP in two scenarios.

The contribution values of each driving factor to various types of land use expansion are exhibited in Figure 4.

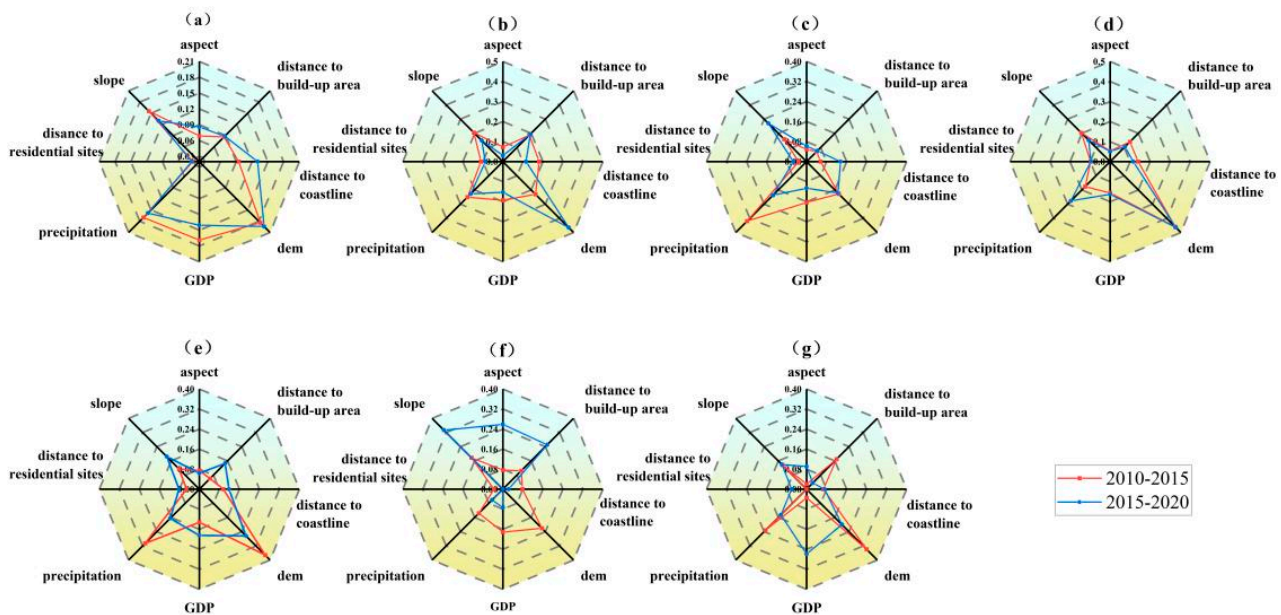


Figure 4. The distribution of each driving factor. (a) the distribution of each driving factor to cropland; (b) the distribution of each driving factor to forest; (c) the distribution of each driving factor to grassland; (d) the distribution of each driving factor to waterarea; (e) the distribution of each driving factor to bareland; (f) the distribution of each driving factor to construction land; (g) the distribution of each driving factor to wetland.

4. Results

4.1. The Change of the LUCC

The evolution of the LUCC in the southeastern coastal area from 1990 to 2020 is presented in Figure 5. However, the rate of urbanization remains high under the influence of the NCSSCP. From an overall perspective, the rate of development of forests far exceeds the rate of afforestation. In terms of different time series, the impact of the NCSSCP is also different at each stage. Under the first phase of the NCSSCP, forest increased by 1.1%, and construction land increased by 101.3%. Cropland decreased by 9.9%, and grassland decreased by 68.2%. These results suggested that the first phase of the NCSSCP had a great impact on LUCC and changed the geomorphic characteristics and spatial pattern with the economic development and urbanization rate of the southeastern coastal area. The decrease in grassland and bare land indicated that the utilization rate of land was improved. From 2000 to 2010, it was the second phase of the NCSSCP in the southeastern coastal area. China's economic growth achieved a great leap up until 2015. Thus, construction land increased by 75.3%, maintaining a high growth rate. The possession amount was 95.2%, while forest decreased by 1.1%, and was mainly converted to cropland and construction land.

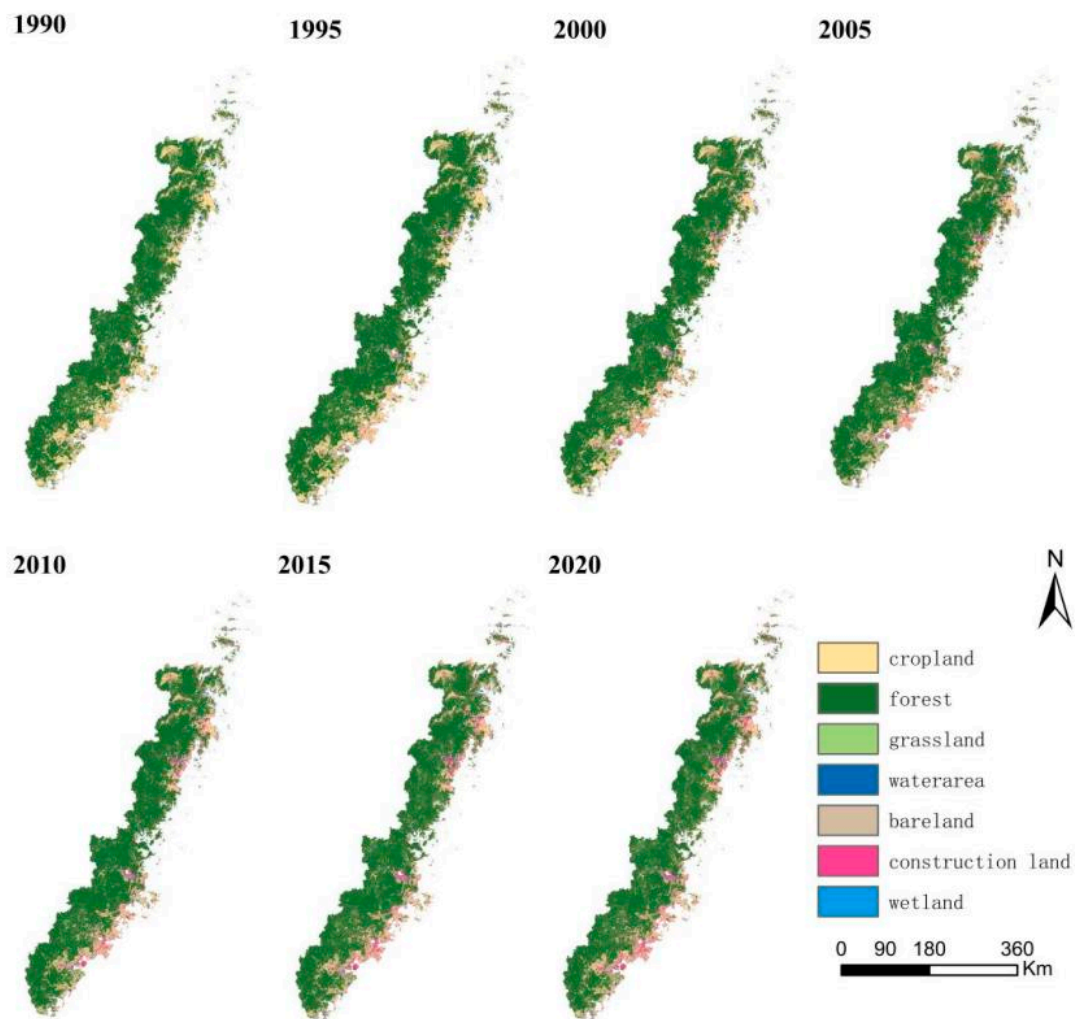


Figure 5. The spatiotemporal evolution of the LUCC in the southeastern coastal area.

The increase of the area of the conversion of cropland to forest was not as fast as forest exploitation, with a deficit of 507.16 km². The urbanization process and its irreversibility deprived the expansion and development of other land-use types, especially forest. By 2020, the preliminary phase of the third phase had been completed, whereas its effect was not significant due to the development of urbanization. However, cropland should meet a certain level in order to match the economic growth. Therefore, the behavior of exploiting forest for farmland reduced a large area of the forest land. In essence, it is the effect of urbanization in other forms. Forest decreased by 1.8%, and its possession decreased to 93.4%. The total area of forest was still in a declining trend, and the deficit of cropland reached 2523.22 km². Forest was still not well protected even under the influence of the NCSSCP. Cropland increased by 4.1%, owing to the use of forest and water. Compared with the end of the second phase, construction land increased by 11.4%, still maintaining a consistent growth rate. Simultaneously, wetland grew steadily, increasing by 192.9% and 17.6% compared with 1990 and 2000, respectively. Under the influence of ecological wetland protection, the wetland has been restored well. The LUCC transfer matrix is presented in Table 4.

Table 4. The LUCC transfer matrix of the whole coastal shelterbelt system construction project.

The First Phase of the NCSSCP		2000						
1990	cropland	cropland	forest	grassland	water area	bare land	construction land	wetland
	forest	16,639,270 *	3,338,626	24,168	411,278	2320	1,756,732	4739
	grassland	2,657,734	61,317,184 *	16,739	56,751	163	101,676	327
	water area	102,678	57,675	31,231 *	7001	4510	55,355	11
	bare land	251,083	75,423	3147	1,605,966 *	2028	136,339	5878
	construction land	7684	316	2384	3043	12,430 *	8704	1
	wetland	286,889	40,442	3599	80,043	1012	1,207,111 *	538
		1995	275	82	1906	68	541	205 *
The second phase of the NCSSCP		2015						
2000	cropland	cropland	forest	grassland	water area	bare land	construction land	wetland
	forest	15,167,729 *	2,360,134	21,586	350,968	4758	2,089,479	1196
	grassland	2,923,649	61,741,638 *	9203	9821	320	188,344	0
	water area	28,025	18,453	18,613 *	3355	1733	12,502	0
	bare land	215,173	18,425	3150	1,707,161 *	6459	270,622	1461
	construction land	5064	87	644	5545	5201 *	7209	0
	wetland	11,104	330	49	82,786	147	3,189,999 *	0
		96	3	1	31	0	84	13,688 *
The early stage of the third phase of the NCSSCP		2020						
2015	cropland	cropland	forest	grassland	water area	bare land	construction land	wetland
	forest	13,450,195 *	2,803,576	11,003	224,050	3912	1,790,566	4419
	grassland	3,867,695	59,896,011 *	8319	107,470	334	184,443	587
	water area	19,594	13,533	3814 *	1864	900	12,116	125
	bare land	393,732	91,315	2994	1,380,425 *	3740	201,203	5643
	construction land	5038	238	553	993	3868 *	7067	16
	wetland	1,300,542	131,975	3372	106,786	4076	4,165,309 *	2284
		3585	429	123	4884	1	2252	1858 *

* The symbol * represents the possession amount of each land use type.

4.2. Landscape Pattern Index Analysis

In this paper, six indices, including landscape fragmentation indexes (LSI, CONTAG, and DIVISION) and landscape diversity indexes (SHEI, SHDI, and AI) were selected in order to analyze the LUCC and spatial pattern of the coastal shelterbelt in the southeastern coastal area. Figure 6 demonstrates the changes in the two dimensions' indices from 1985 to 2020. Generally, LSI, SHEI, and SHDI exhibited an increasing trend, while CONTAG, DIVISION, and AI showed a downward trend. The landscape fragmentation index reflected the fragmentation and complexity of the NCSSCP in the southeastern coastal area. The improvement of the LSI index indicated that the shape of the LUCC in the southeastern coastal area was more irregular. The patch edge was intricate, and the degree of landscape fragmentation increased. The decrease of the CONTAG index suggested that the extent of land species sprawl decreased, and the interaction among different land species was fragmented. The decrease of DIVISION implied that the spread of land types in the southeastern coastal area was reduced, and the interaction of different land types was fragmented. Meanwhile, the degree of separation and discretization decreased. The landscape diversity index reflected the diversity and complexity of land use and land cover under the effect of the NCSSCP in the southeastern coastal area. The growth of the SHDI index and SHEI index revealed the spatial diversity and complexity of the southeastern coastal area. The decrease in the AI index represented the decline of the agglomeration of the same land type in the southeastern coastal area. The LUCC implied a trend of diversification under the interaction of different land types.

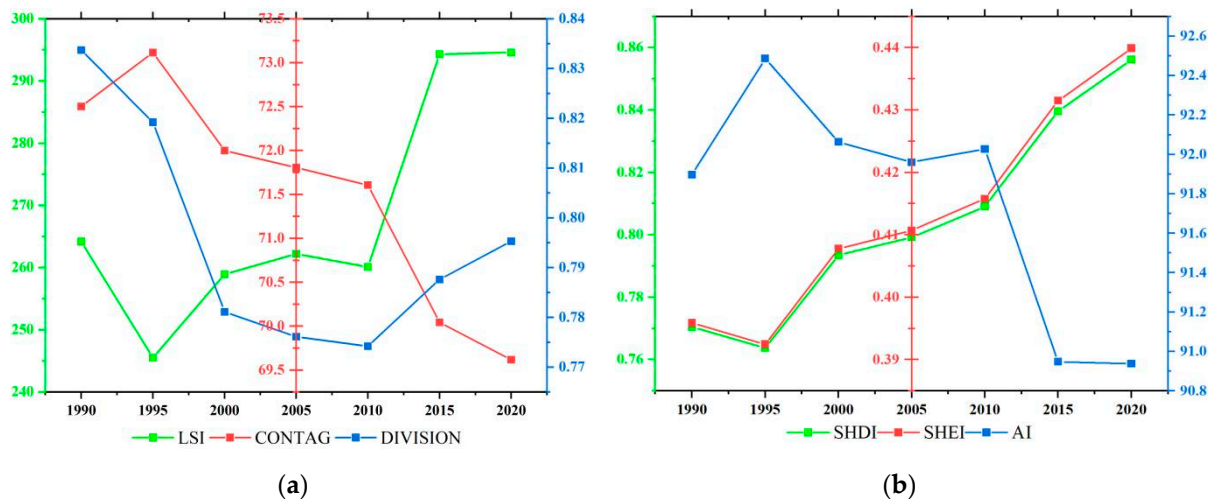


Figure 6. (a) The evolution of the landscape pattern index from 1990 to 2020 in the southeastern coastal area, including LSI, CONTAG and DIVISION. (b) The evolution of the landscape pattern index from 1990 to 2020 in the southeastern coastal area, including SHDI, SHEI and AI.

4.3. Scenario Setting and Analysis

4.3.1. The LUCC Analysis of the Scenarios

Two scenarios of inertial development and goal-orientation are set in this paper. The inertial development scenario (S1) takes the remote sensing images of the LUCC in 2015 and 2020, and the Markov model is employed to simulate and predict the land use and land cover demand in 2025. S1 is set by the principle of business as usual; that is, each type of land use would require development as the inertial trend. The Markov-PLUS model is coupled to combine both quantity and spatial prediction in order to simulate the spatiotemporal LUCC evolution in the southeastern coastal area. The goal-oriented scenario (S2) is set according to the target of the afforestation area proposed in the NCSSCP. The amount of forest area is extracted and quantified as the land demand, in order to simulate the LUCC once the third phase of the NCSSCP has been completed, so as to indicate differences in land use and land cover between S1 and S2. The comparison of

the results is illustrated in Figure 7 ((a) the inertia development scenario—S1; (b) the goal-oriented scenario—S2). In other words, whether the goal of the NCSSCP can be completed can be determined according to the inertial trend of the preliminary development of the NCSSCP in the southeastern coastal area from 2015 to 2020. However, such situations can be visualized and displayed in space.

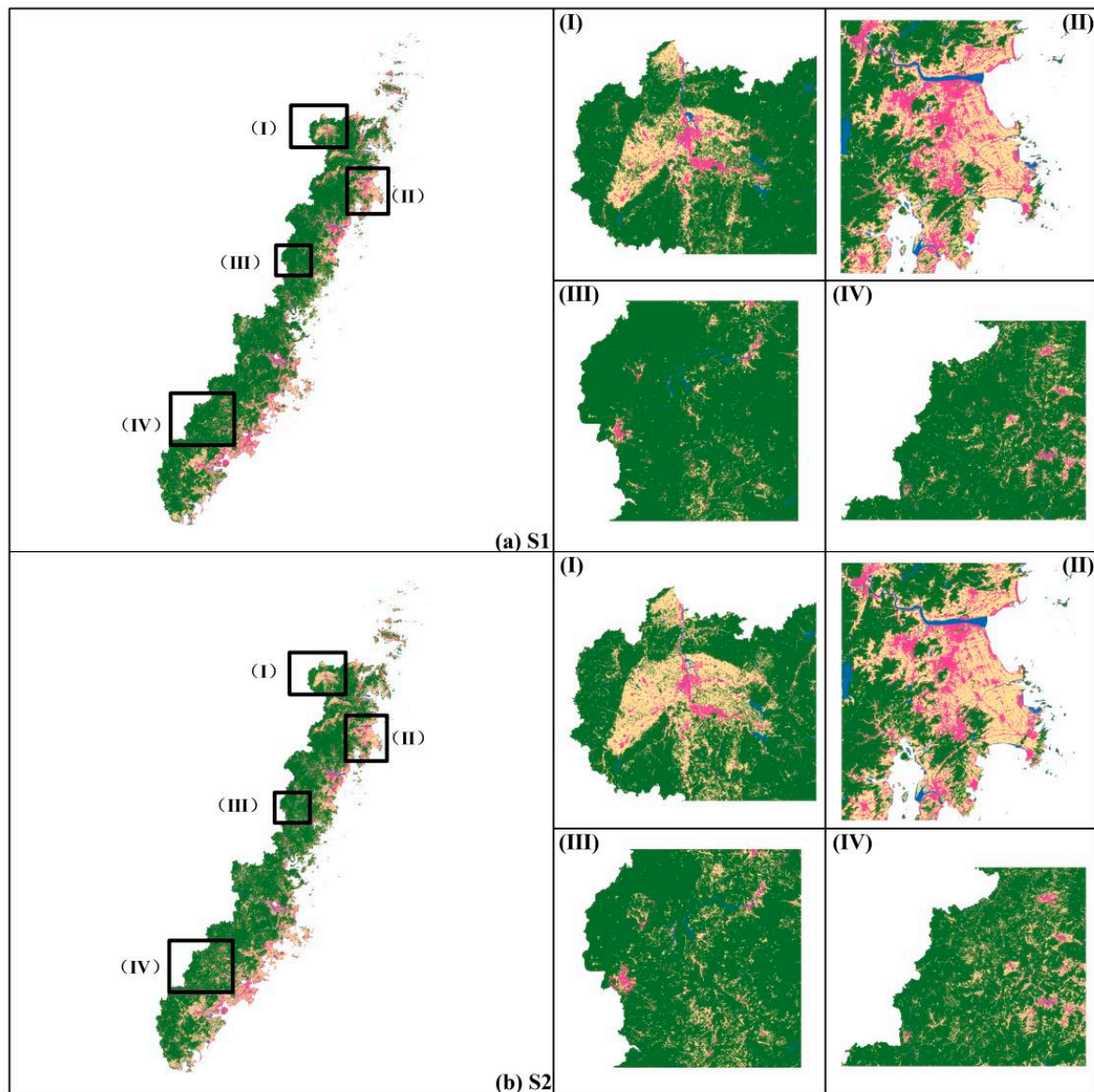


Figure 7. (a) The result of the LUC under S1 in the southeastern coastal area in 2025. (I–IV) are the four corners of the results. (b) The result of the LUC under S2 in the southeastern coastal area in 2025. (I–IV) in the S2 are the same corners, respectively corresponding to S1.

The differences between the inertia development scenario and the goal-oriented scenario are shown in Figure 6. The differences of the LUC results in the district are mainly distributed in four areas, among which (a) and (e) are distributed in the northern area of the southeastern coastal area, (b) and (f) are distributed in the northeast area of the southeastern coastal area, (c) and (g) are distributed in the central area of the southeastern coastal area, and (d) and (h) are distributed in the southern area of the southeastern coastal area.

Under S1, the forest is still in a state of continuous reduction. Compared with 2015, forest decreased by 2.9%, and the possession amount of forest was 95.9%. Under S1, the

forest was not well maintained and restored, while cropland extended the growth trend from 2015 to 2020, with an increase of 564.03 km² compared with 2020. Besides this, about 65.8% of the cropland was transferred from the forest, as the behavior of “exploiting forests and creating cropland” is the main source of the growth of cropland. The construction land increased by 1.29%, with a total increase of 74.54 km². Under S1, the forest was used to reclaim a large amount of cropland, and was then expropriated and built into construction land, which is the most direct embodiment of urbanization’s influence. Forest decreased by about 633.19 km², contrary to the goal of the NCSSCP, namely, creating about 1666.12 km² of forest. According to the development trend, ecological protection was ignored. Such a development trend runs counter to the NCSSCP’s development philosophy, making it impossible to complete the goal.

Under S2, the forest was well restored and increased, with a total increase of 1666.12 km², which was 2.94% higher than that in 2020. The ecological value of the NCSSCP in the southeastern coastal area was truly revealed. Meanwhile, the cropland was effectively used and controlled at a decrease of 10.06% compared with 2015. Additionally, ecological restoration was significantly promoted owing to the NCSSCP and the project of returning cropland to forest. Construction land increased by 24.1% compared with 2015, with an increase of 11.4% compared to 2020. The speed of the process of urbanization is still at a high level. However, the afforestation speed matches the speed of urbanization and the economy. Ecological restoration is emphasized under S2. Moreover, the southeastern coastal area achieved high-quality development with the balance of ecology and economic development.

4.3.2. The Landscape Pattern Index Analysis

Under the two scenarios, the landscape pattern index evolution in the southeastern coastal area is depicted in Figure 8. Specifically, (a) consists of the LSI index, CONTAG index, and DIVISION index in the landscape fragmentation index, mainly reflecting the fragmentation and the complexity of the landscape pattern and spatial structure of the LUCC patches in the southeastern coastal area, and (b) demonstrates the landscape diversity index, including SHDI, SHEI, and AI, suggesting the degree of diversity of the LUCC patches in the southeastern coastal area and the interaction between different land types.

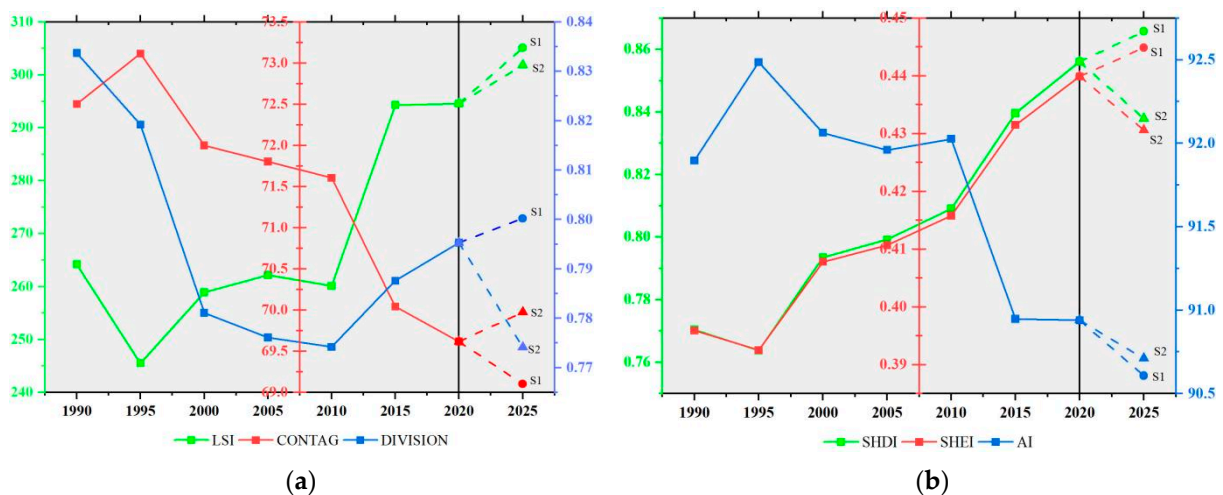


Figure 8. (a) Evolution and prediction of the landscape pattern index in both scenarios, including LSI, CONTAG and DIVISION. (b) Evolution and prediction of the landscape pattern index in both scenarios, including SHDI, SHEI and AI.

Under the scenario of S1, the LSI index increased, implying that the fragmentation in the southeastern coastal area became higher. The mutual transformation degree between land types was higher. The CONTAG index was inversely proportional to the degree of fragmentation, and its downward trend reflected the wide distribution of various types

of land. The increase of the DIVISION index confirmed the increase in separation and fragmentation, and the spatial structure was complicated. The increase of SHDI and SHEI index demonstrated the increase in the diversity of landscape patterns, showing a richer diversity compared to 2020. The AI index was inversely proportional to the diversity, and its downward trend revealed a decrease in the aggregation of various species and an increase in diversity.

Under the scenario of S2, the LSI still presented an upward trend, and the conversion degree between cropland and forest was still high. Nonetheless, the rise of the CONTAG index indicated that the spatial structure and landscape pattern of the southeastern coastal areas increased with the deepening of the NCSSCP. The land types were scattered and clustered. The decline of the DIVISION index manifested the decrease of separation of the landscape pattern in the southeastern coastal areas, as well as the decrease in the degree of fragmentation of the spatial structure. Compared with 2020, SHDI and SHEI decreased, revealing that the diversity of landscape patterns in the southeastern coastal area was lower than that of 2020, and the interaction between different types was small. Compared with the S1 scenario, the AI index was on an upward trend. Thus, the aggregation among land types was on the rise under S2.

5. Discussion

5.1. Simulation Result Analysis

The southeastern coastal area encounters the most frequent natural disasters. Thus, NCSSCP is a critical part of China's "two screens and three belts" strategy to protect coastal ecological security. The impact analysis of the NCSSCP and the prediction of the future changes in LUCC can provide scientific advice for the overall planning of land and sea and the proper rational configuration of land resources, contributing to the follow-up development of the NCSSCP. This study selected the PLUS model and set two scenarios to predict the LUCC in 2025, which have a high accuracy in the simulation of the spatiotemporal evolution of the LUCC [38].

Based on remote sensing images of the LUCC from 2010 to 2015, this research used the PLUS model to simulate the LUCC in 2020, and used the Kappa coefficient to verify the accuracy. The results show that the PLUS model has very high spatial simulation ability, and can show the changes of the LUCC in time and space, coupled with the Markov model. The PLUS model can be applied to LUCC simulation. Therefore, two scenarios were set up to analyze the future LUCC and predict the landscape pattern and spatial structure of southeastern coastal areas under different land resource management strategies.

5.2. Management Strategies for the Future Development of Land Resources

Under S1, the forest is mainly transferred out to cropland. The ecological protection capacity is reduced, while construction land is expands rapidly. The restoration of the ecological environment is slow, while the construction land expands rapidly with more diverse and complex spatial structures. As a result, the ecological environment in the southeastern coastal areas will be damaged, hindering the sustainable development of ecological restoration projects.

Under S2, the ecological environment of the southeastern coastal area is restored, and the ecological environment was well protected. The speed of afforestation matches the expansion speed of the construction land, and the spatial pattern is more agglomerated. Completing the goal of the NCSSCP in the southeastern coastal area can contribute to the provision of guidance to sustainable development, which is of great significance to displaying the spatial visualization of the LUCC.

Such different scenarios and land resource management strategies can provide a contrasting context for decision-makers to promote sustainable development. As suggested by the development trend of the NCSSCP from 2015 to 2020 and the simulation results analyzed by the different scenarios, the following suggestions can be provided.

- Continue to implement the NCSSCP and expand the total amount of forest resources in southeastern coastal areas. The implementation of the “Belt and Road” strategy and the concept of green development can be comprehensively promoted. Continuing the NCSSCP in the southeastern area is urgent for the further enhancement of the quality of the ecological environment and the acceleration of the construction of ecological civilization.
- It is also necessary to further facilitate the afforestation and promote the greening construction of cities and their surroundings through scientific and effective means of construction and management. In southeastern coastal areas, the protection of shelterbelts should be strengthened in order to improve the disaster prevention.
- Further improving forest coverage and increasing forest carbon sink can offset some industrial greenhouse gas emissions and reduce China’s total pollution. This is a crucial measure in order to actively respond to global warming.
- The industrial structure of the southeastern coastal area should accelerate the change of the first industry to secondary and tertiary industries. NCSSCP should focus on achieving a net forest increase, as opposed to focusing on afforestation, which seems plausible but has an insufficient forest area due to urbanization. The ecological environment should be considered in the process of economic development in the southeastern coastal area.
- The ecological system should be made more stable in order to promote sustainable development. The landscape pattern and spatial structure of the southeastern coastal area are relatively simple and complete. This indicates that the interaction between various types of land use should be elementary. Therefore, the following development should be clustered according to the landscape analysis.

5.3. Deficiencies and Prospects

The main limitation of this paper is that the LUCC dataset used was not detailed enough. In other words, all of the evergreen broad-leaved, evergreen coniferous, deciduous broad-leaved and deciduous coniferous forests were classified into a unified type of forest. Although the LUCC can reflect the temporal and spatial evolution of forests, only a brief description can be provided. Additionally, the LUCC dataset does not match the types of forest land constructed in the NCSSCP, making it difficult to perform more in-depth planning and discussion. During the simulation, the driving factors were selected from the perspective of the natural environment and socioeconomics. Nevertheless, there are some limitations and one-sidedness. The research only stops at the spatio-temporal evolution of the ecological pattern.

Economic development, the ecological environment, and sustainable development should be considered simultaneously in the future development of the southeastern coastal area. This lays a scientific foundation for the achievement of balanced development between economic growth and ecological security. In future research, field research and sampling should be conducted, and various remote sensing technologies will be adopted to analyze the ecological functions and service value under the evolution of the LUCC in the southeastern coastal areas.

6. Conclusions

Since the first phase of the coastal shelterbelt system construction project in the southeastern coastal area in 1990, the forest has been restored, and the ecology has been effectively protected. However, the rate of the return of farmland to forest was sluggish, as the rate of forest development was slower than the speed of the economy’s development. Consequently, the amount of forest exhibited a declining trend. In the process of urbanization, the rate of forest development and the rate of the development of construction land were rapid.

From 1990 to 2020 (the first phase to the early stage of the third phase of the NCSSCP in the southeastern coastal area), the landscape pattern and spatial structure were fragmented and diversified, with irregular and discordant patch edges. The interaction between

various land-use types was strengthened with the acceleration of economic growth and urbanization. Meanwhile, the landscape connectivity was reduced. Therefore, the spatial structure was highly discretized and fragmented, with poor stability, and the ecology was damaged to a certain extent.

In the process of implementation, the shelterbelt system project only stresses the plantation of the forest, while neglecting the reduction of forest land caused by the urbanization process. Consequently, the net growth of the forest area in a real sense cannot be achieved, resulting in a waste of resources and ecological imbalance.

Under the two simulation scenarios, the LUCC in the southeastern coastal area shows different development situations. In the case of S1, the spatial structure of the LUCC is fragmented and separated. The urbanization rate is high, but the ecology is not stable or safe enough. In the S2, the spatial structure of the LUCC is more agglomerated, and the forest area achieves a net increase.

Through the comparative analysis of the two scenarios, according to the current development trend (a severe forest deficit), the goal of the NCSSCP cannot be achieved. Meanwhile, through the visual analysis of the LUCC, it was shown to be conducive to the sustainable development of the NCSSCP, and to provide spatial visualization guidance for subsequent development.

The most suitable land resource management and strategic planning for the southeastern coast should not only accomplish the afforestation goals of the NCSSC but also achieve the net growth of forest land; that is, the speed of afforestation should exceed the speed of urbanization. Such a strategy can achieve high-quality development that takes into account both economic benefits and ecological security.

Author Contributions: All of the authors significantly contributed to this study. F.Y. proposed the idea and designed the experiments. S.B. wrote the manuscript and processed the data. All authors have read and agreed to the published version of the manuscript.

Funding: This paper was jointly supported by the National Natural Science Foundation of China (Grant No. 42001235) and the Science and Technology Plan Program of Zhoushan (Grant No. 2021C21022).

Institutional Review Board Statement: Not applicable.

Informed Consent Statement: Not applicable.

Data Availability Statement: The data that support the findings of this study are available from the corresponding author (F.Y.) upon justifiable request.

Conflicts of Interest: The authors declare no conflict of interest.

References

1. Jiang, P.; Cheng, L.; Li, M.; Zhao, R.; Duan, Y. Impacts of LUCC on soil properties in the riparian zones of desert oasis with remote sensing data: A case study of the middle Heihe River basin, China. *Sci. Total Environ.* **2015**, *506–507*, 259–271. [[CrossRef](#)] [[PubMed](#)]
2. Faruque, M.J.; Vekerdy, Z.; Hasan, M.Y.; Islam, K.Z.; Young, B.; Ahmed, M.T.; Monir, M.U.; Shovon, S.M.; Kakon, J.F.; Kundu, P. Monitoring of land use and land cover changes by using remote sensing and GIS techniques at human-induced mangrove forests areas in Bangladesh. *Remote Sens. Appl. Soc. Environ.* **2022**, *25*, 100699. [[CrossRef](#)]
3. National Coastal Shelterbelt System Construction Project Planning. 2017. Available online: <http://www.gov.cn/xinwen/2017-05/16/5194348/files/8cfb540b5ff744518f1f05abdd201bdd.pdf> (accessed on 1 March 2022).
4. Zou, L.; Liu, Y.; Wang, J.; Yang, Y. An analysis of land use conflict potentials based on ecological-production-living function in the southeast coastal area of China. *Ecol. Indic.* **2021**, *122*, 107297. [[CrossRef](#)]
5. Zou, J.; Lu, N.; Jiang, H.; Qin, J.; Yao, L.; Xin, Y.; Su, F. Performance of air temperature from ERA5-Land reanalysis in coastal urban agglomeration of Southeast China. *Sci. Total Environ.* **2022**, *828*, 154459. [[CrossRef](#)] [[PubMed](#)]
6. Xiong, L.; Xi, B.; Wu, Y.; Liu, S.; Zhang, L.; Huang, X.; Macreadie, P.I. Nutrient input estimation and reduction strategies related to land use and landscape pattern (LULP) in a near-eutrophic coastal bay with a small watershed in the South China sea. *Ocean Coast. Manag.* **2021**, *206*, 105573. [[CrossRef](#)]
7. Zou, L.; Liu, Y.; Wang, J.; Yang, Y.; Wang, Y. Land use conflict identification and sustainable development scenario simulation on China's southeast coast. *J. Clean. Prod.* **2019**, *238*, 117899. [[CrossRef](#)]

8. Zong, S.; Hu, Y.; Zhang, Y.; Wang, W. Identification of land use conflicts in China's coastal zones: From the perspective of ecological security. *Ocean Coast. Manag.* **2021**, *213*, 105841. [[CrossRef](#)]
9. Tian, Z.; Liu, F.; Liang, Y.; Zhu, X. Mapping soil erodibility in southeast China at 250 m resolution: Using environmental variables and random forest regression with limited samples. *Int. Soil Water Conserv. Res.* **2022**, *10*, 62–74. [[CrossRef](#)]
10. Zhang, F.; Yang, X. Improving land cover classification in an urbanized coastal area by random forests: The role of variable selection. *Remote Sens. Environ.* **2020**, *251*, 112105. [[CrossRef](#)]
11. Ji, Y.; Jin, J.; Zhu, Q.; Zhou, S.; Wang, Y.; Wang, P.; Xiao, Y.; Guo, F.; Lin, X.; Xu, J. Unbalanced forest displacement across the coastal urban groups of eastern China in recent decades. *Sci. Total Environ.* **2020**, *705*, 135900. [[CrossRef](#)]
12. Xie, H.; Wang, G.G.; Yu, M. Ecosystem multifunctionality is highly related to the shelterbelt structure and plant species diversity in mixed shelterbelts of eastern China. *Glob. Ecol. Conserv.* **2018**, *16*, e00470. [[CrossRef](#)]
13. Fan, L.; Tarin, M.W.K.; Zhang, Y.; Han, Y.; Rong, J.; Cai, X.; Chen, L.; Shi, C.; Zheng, Y. Patterns of soil microorganisms and enzymatic activities of various forest types in coastal sandy land. *Glob. Ecol. Conserv.* **2021**, *28*, e01625. [[CrossRef](#)]
14. Liu, Y.; Xu, N.; Li, Z.; Wang, J.; Zeng, H. Differential impact of constructed land expansion on ecosystem health: A case study in the coastal region of the East China Sea. *Ecol. Eng.* **2022**, *180*, 106665. [[CrossRef](#)]
15. Zhang, X.; Zhou, Y.; He, W.; Ju, W.; Liu, Y.; Bi, W.; Cheng, N.; Wei, X. Land cover change instead of solar radiation change dominates the forest GPP increase during the recent phase of the Shelterbelt Program for Pearl River. *Ecol. Indic.* **2022**, *136*, 108664. [[CrossRef](#)]
16. Li, Z.; Wang, J.; Kong, X.; Zhang, B.; Liu, J.; Ding, S.; Du, Y. Effects of ecosystems preservation on economic growth in China's coastal region: Multilevel modelling and exploration. *Ecol. Indic.* **2021**, *132*, 108224. [[CrossRef](#)]
17. Liu, C.; Yang, M.; Hou, Y.; Xue, X. Ecosystem service multifunctionality assessment and coupling coordination analysis with land use and land cover change in China's coastal zones. *Sci. Total Environ.* **2021**, *797*, 149033. [[CrossRef](#)]
18. Lopez-Carr, D.; Davis, J.; Jankowska, M.; Grant, L.; Lopez-Carr, A.C.; Clark, M. Space versus Place in Complex Human-Natural Systems: Spatial and Multi-level Models of Tropical Land Use and Cover Change (LUCC) in Guatemala. *Ecol. Model.* **2012**, *229*, 64–75. [[CrossRef](#)]
19. Song, K.; Zhao, J.; Ouyang, W.; Zhang, X.; Hao, F. LUCC and landscape pattern variation of wetlands in warm-rainy Southern China over two decades. *Procedia Environ. Sci.* **2010**, *2*, 1296–1306. [[CrossRef](#)]
20. Wang, H.; Zhang, C.; Yao, X.; Yun, W.; Ma, J.; Gao, L.; Li, P. Scenario simulation of the tradeoff between ecological land and farmland in black soil region of Northeast China. *Land Use Policy* **2022**, *114*, 105991. [[CrossRef](#)]
21. Gomes, E.; Banos, A.; Abrantes, P.; Rocha, J.; Schlapfer, M. Future land use changes in a peri-urban context: Local stakeholder views. *Sci. Total Environ.* **2020**, *718*, 137381. [[CrossRef](#)]
22. Ye, L.; Yang, D.; Dang, Y.; Wang, J. An enhanced multivariable dynamic time-delay discrete grey forecasting model for predicting China's carbon emissions. *Energy* **2022**, *249*, 123681. [[CrossRef](#)]
23. Esgalhado, C.; Guimarães, M.H.; Lardon, S.; Debolini, M.; Balzan, M.V.; Gennai-Schott, S.C.; Simón Rojo, M.; Mekki, I.; Bouchemal, S. Mediterranean land system dynamics and their underlying drivers: Stakeholder perception from multiple case studies. *Landsc. Urban Plan.* **2021**, *213*, 104134. [[CrossRef](#)]
24. Hu, X.; Luo, H.; Guo, M.; Wang, J. Ecological technology evaluation model and its application based on Logistic Regression. *Ecol. Indic.* **2022**, *136*, 108641. [[CrossRef](#)]
25. Sylvester, J. The cover time of a (multiple) Markov chain with rational transition probabilities is rational. *Stat. Probab. Lett.* **2022**, *187*, 109534. [[CrossRef](#)]
26. Basse, R.M.; Omrani, H.; Charif, O.; Gerber, P.; Bódis, K. Land use changes modelling using advanced methods: Cellular automata and artificial neural networks. *The spatial and explicit representation of land cover dynamics at the cross-border region scale. Appl. Geogr.* **2014**, *53*, 160–171. [[CrossRef](#)]
27. Huang, W.; An, Y.; Pan, Y.; Li, J.; Chen, C. Predicting transient particle transport in periodic ventilation using Markov chain model with pre-stored transition probabilities. *Build. Environ.* **2022**, *211*, 108730. [[CrossRef](#)]
28. Mokarram, M.; Pham, T.M. CA-Markov model application to predict crop yield using remote sensing indices. *Ecol. Indic.* **2022**, *139*, 108952. [[CrossRef](#)]
29. Zhao, M.; He, Z.; Du, J.; Chen, L.; Lin, P.; Fang, S. Assessing the effects of ecological engineering on carbon storage by linking the CA-Markov and InVEST models. *Ecol. Indic.* **2019**, *98*, 29–38. [[CrossRef](#)]
30. Zhang, Y.; Li, Y.; Lv, J.; Wang, J.; Wu, Y. Scenario simulation of ecological risk based on land use/cover change—A case study of the Jinghe county, China. *Ecol. Indic.* **2021**, *131*, 108176. [[CrossRef](#)]
31. Zeng, L.; Liu, X.; Li, W.; Ou, J.; Cai, Y.; Chen, G.; Li, M.; Li, G.; Zhang, H.; Xu, X. Global simulation of fine resolution land use/cover change and estimation of aboveground biomass carbon under the shared socioeconomic pathways. *J. Environ. Manag.* **2022**, *312*, 114943. [[CrossRef](#)]
32. Geng, J.; Shen, S.; Cheng, C.; Dai, K. A hybrid spatiotemporal convolution-based cellular automata model (ST-CA) for land-use/cover change simulation. *Int. J. Appl. Earth Obs. Geoinf.* **2022**, *110*, 102789. [[CrossRef](#)]
33. Xie, L.; Wang, H.; Liu, S. The ecosystem service values simulation and driving force analysis based on land use/land cover: A case study in inland rivers in arid areas of the Aksu River Basin, China. *Ecol. Indic.* **2022**, *138*, 108828. [[CrossRef](#)]
34. Yang, J.; Huang, X. The 30 m annual land cover dataset and its dynamics in China from 1990 to 2019. *Earth Syst. Sci. Data* **2021**, *13*, 3907–3925. [[CrossRef](#)]

35. McGarigal, K.; Marks, B.J. FRAGSTATS: Spatial Pattern Analysis Program for Quantifying Landscape Structure; 1995. Available online: https://www.fs.fed.us/pnw/pubs/pnw_gtr351.pdf (accessed on 22 March 2022).
36. Shehab, Z.N.; Jamil, N.R.; Aris, A.Z.; Shafie, N.S. Spatial variation impact of landscape patterns and land use on water quality across an urbanized watershed in Bentong, Malaysia. *Ecol. Indic.* **2021**, *122*, 107254. [[CrossRef](#)]
37. Fu, F.; Deng, S.; Wu, D.; Liu, W.; Bai, Z. Research on the spatiotemporal evolution of land use landscape pattern in a county area based on CA-Markov model. *Sustain. Cities Soc.* **2022**, *80*, 103760. [[CrossRef](#)]
38. Liang, X.; Guan, Q.; Clarke, K.C.; Liu, S.; Wang, B.; Yao, Y. Understanding the drivers of sustainable land expansion using a patch-generating land use simulation (PLUS) model: A case study in Wuhan, China. *Comput. Environ. Urban Syst.* **2021**, *85*, 101569. [[CrossRef](#)]
39. Li, C.; Wu, Y.; Gao, B.; Zheng, K.; Wu, Y.; Li, C. Multi-scenario simulation of ecosystem service value for optimization of land use in the Sichuan-Yunnan ecological barrier, China. *Ecol. Indic.* **2021**, *132*, 108328. [[CrossRef](#)]
40. Jiang, Y.; Huang, M.; Chen, X.; Wang, Z.; Xiao, L.; Xu, K.; Zhang, S.; Wang, M.; Xu, Z.; Shi, Z. Identification and risk prediction of potentially contaminated sites in the Yangtze River Delta. *Sci. Total Environ.* **2022**, *815*, 151982. [[CrossRef](#)]
41. Han, J.; Hu, Z.; Mao, Z.; Li, G.; Liu, S.; Yuan, D.; Guo, J. How to Account for Changes in Carbon Storage from Coal Mining and Reclamation in Eastern China? Taking Yanzhou Coalfield as an Example to Simulate and Estimate. *Remote Sens.* **2022**, *14*, 2014. [[CrossRef](#)]
42. Xu, L.; Liu, X.; Tong, D.; Liu, Z.; Yin, L.; Zheng, W. Forecasting Urban Land Use Change Based on Cellular Automata and the PLUS Model. *Land* **2022**, *11*, 652. [[CrossRef](#)]
43. Kurnia, A.A.; Rustiadi, E.; Fauzi, A.; Pravitasari, A.E.; Saizen, I.; Ženka, J. Understanding Industrial Land Development on Rural-Urban Land Transformation of Jakarta Megacity's Outer Suburb. *Land* **2022**, *11*, 670. [[CrossRef](#)]
44. Zhai, H.; Lv, C.; Liu, W.; Yang, C.; Fan, D.; Wang, Z.; Guan, Q. Understanding Spatio-Temporal Patterns of Land Use/Land Cover Change under Urbanization in Wuhan, China, 2000–2019. *Remote Sens.* **2021**, *13*, 3331. [[CrossRef](#)]
45. Li, C.; Yang, M.; Li, Z.; Wang, B. How Will Rwandan Land Use/Land Cover Change under High Population Pressure and Changing Climate? *Appl. Sci.* **2021**, *11*, 5376. [[CrossRef](#)]
46. Shi, M.; Wu, H.; Fan, X.; Jia, H.; Dong, T.; He, P.; Baqa, M.F.; Jiang, P. Trade-Offs and Synergies of Multiple Ecosystem Services for Different Land Use Scenarios in the Yili River Valley, China. *Sustainability* **2021**, *13*, 1577. [[CrossRef](#)]